Plate tearing in the northwestern corner of the subducting Philippine Sea Plate

Jing-Yi Lin [a,*], Shu-Kun Hsu [a], Jean-Claude Sibuet [a], Chao-Shing Lee [b], Chin-Wei Liang [b]

[a] Institute of Geophysics, National Central University, 300 Jhongda Road, Jhongli City, Taoyuan County 32001, Taiwan
[b] Institute of Applied Geophysics, National Taiwan Ocean University, 2 Pei-Ning Road, Keelung 202, Keelung, Taiwan

ABSTRACT

The Philippine Sea Plate (PHS) simultaneously subducts northwestward and collides eastward with the Eurasian Plate (EU) in northeast Taiwan. These two tectonic events induce high seismic activity, which makes northeastern Taiwan one of the most seismically active zones in the world. To understand the mechanical processes at work, we used existing geophysical data and the aftershocks recorded following a recent large strike-slip event occurring within the PHS oceanic crust. During this event, a NW–SE trending left-lateral sub-parallel to the PHS/EU convergence vector was active. As a consequence of the collision/subduction plate geometry, we show that the lithosphere of the northwestern corner of the PHS has been torn in a NW–SE orientation. This tectonic feature is associated with an abrupt tectonic stress boundary and could generate large intra-plate earthquakes.

© 2013 Elsevier Ltd. All rights reserved.

1. Introduction

The Philippine Sea Plate (PHS) moves northwestward (Yu et al., 1997) (ca. N306°-312°) relative to the Eurasian Plate (EU), with an 8–9 cm/yr PHS/EU plate convergence vector near Taiwan. The northwestern corner of the PHS subducts northward beneath the Ryukyu arc and collides westward with the EU margin, creating the Taiwan orogen (Fig. 1). The majority of the earthquakes in and around Taiwan is related to the convergence of these two plates (Kao et al., 2000, 1998a; Kao and Jian, 2001; Kubo and Fukuyama, 2003) and characterized by thrust mechanism. However, strike-slip type earthquakes occurring in oblique convergent zones may cause large magnitude earthquakes and create significant damage; an example is the 12 January 2010 Mw 7.0 Haiti earthquake (Hayes et al., 2010; Nettles and Hjorleifsdottir, 2010). In the Ryukyu subduction zone, numerous strike-slip earthquakes have occurred in both the overriding and subducting plates. From August 2009 to April 2010, three large strike-slip earthquakes of magnitude Mw greater than 6.5 occurred beneath the southwestern Ryukyu accretionary wedge (Fig. 1, EQs. 1–3). The earthquake near Okinawa Island had a magnitude of Mw 7.0 and triggered a local tsunami warning (Fig. 1, EQ 1). To understand the earthquake mechanism, we conducted a passive Ocean Bottom Seismometer (OBS) experiment to record the aftershocks approximately three weeks after the 17 August 2009 Mw 6.7 strike-slip type earthquake (Fig. 2a). Based on the aftershocks distribution, combing with

available geophysical data, we aim to establish a tectonic model to adequately explain the observed seismic deformation near the southernmost terminus of the Ryukyu subduction zone next to Taiwan.

2. Data processing and results

A total of 14 OBSs were deployed in a 190 × 50 km area from September 10 to October 2, 2009 by using the research vessel Ocean Research II (ORII). The OBS network covers parts of the Huatung Basin, Gagua Ridge and the southern Ryukyu subduction zone (Fig. 2a). Actually, the initial purpose of this passive active experiment is to study the seismic activity along the Taitung Canyon area located exactly along the OBS array (Fig. 2a). However, after the 17 August 2009 earthquake, we had decided to extend our network further north. This explains why our study area seems to be located at one end of the long narrow network. The OBSs possess a three components velocity type geophone with a natural frequency of 4.5 Hz and one broad-band type hydrophone (Auffret et al., 2004). The spacing between OBSs varied from 25 to 45 km and the sampling frequency of each channel was 128 Hz. Earthquake events were chosen manually from the continuous seismic records. The set of routines of the Boulder Real Time Technologies (BRTTs) ANTELOPE software was used for manual picking of arrival times and preliminary earthquake location. The data were processed with a 1D velocity model obtained from a seismic refraction experiment (Wang et al., 2001) (Fig. 2b), and 514 earthquakes were identified and located (Fig. 3a and b). The magnitude of earthquakes was evaluated by using the duration of seismic waves

Fig. 1. Focal mechanisms from the Global CMT catalog (http://www.globalcmt.org/) from January 1976 to September 2010 plotted on a bathymetric map of the Ryukyu-Taiwan subduction–collision zone. EQs. 1–3 indicate the three large strike-slip earthquakes of magnitude greater than 6.5, which occurred beneath the southwestern Ryukyu accretionary wedge between August 2009 and April 2010. EQ4 shows a recent strike-slip earthquake with Mw 4.49 and a focal depth of 76 km, which occurred on 30 April 2011, beneath the northeastern Taiwan. EU, Eurasia; GR, Gagua Ridge; HB, Huatung Basin; LU, Luzon; LOFZ, Luzon-Okinawa fracture zone; PHS Philippine Sea plate; WPB, West Philippine Basin.
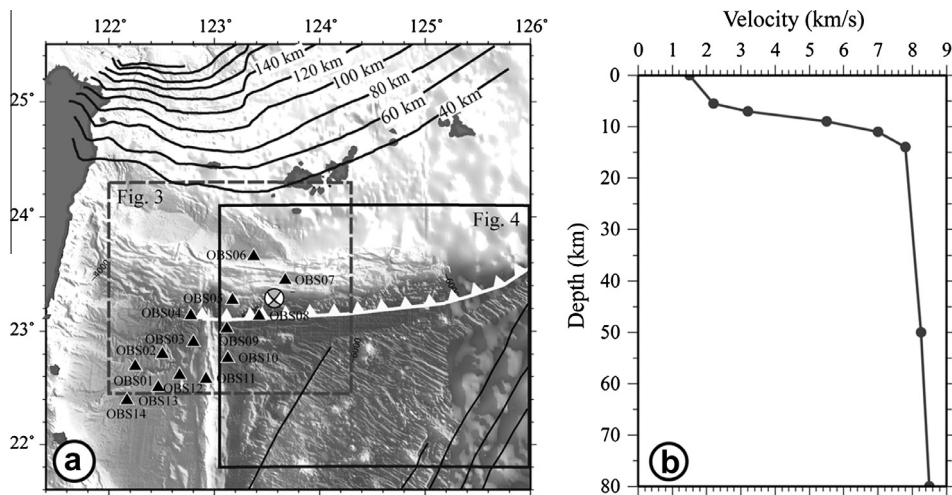

Fig. 2. (a) Shaded bathymetry in the northwestern corner of the PHS (Chang, 2007). Focal mechanism shows the mainshock (17th August 2009 Mw = 6.7 event) in our study. Black triangles are the OBS stations. Gray dashed and black rectangle shows the location of Figs. 3a and c and 4, respectively. Black contours show the slab isobaths determined from the relocated earthquakes (Font et al., 1999). (b) 1-D P-wave velocity model used for the hypocenter determination (gray line) by Wang et al. (2001).

(Tsumura, 1967). The value of magnitude Md for the located earthquakes extends from 2.5 to 5.8. Most Md > 4 events were located beneath the forearc basin area, with hypocenter depth deeper than 60 km and probably originate at the plate interface. Whereas almost all the aftershocks identified from the OBS network were characterized by an Md smaller than three (Fig. 3a). To obtain accurate hypocenter locations, we relocated 336 earthquakes by applying the double-difference method (HypoDD software, Waldhauser and Ellsworth, 2000) to the 514 earthquakes (Fig. 3c and d). The hypoDD technique takes advantage of the fact that if the hypocentral separation between two earthquakes is small compared to the event-station distance and the scale length of velocity heterogeneity, then the ray paths between the source region and a common station are similar along almost the entire ray path. In this case,
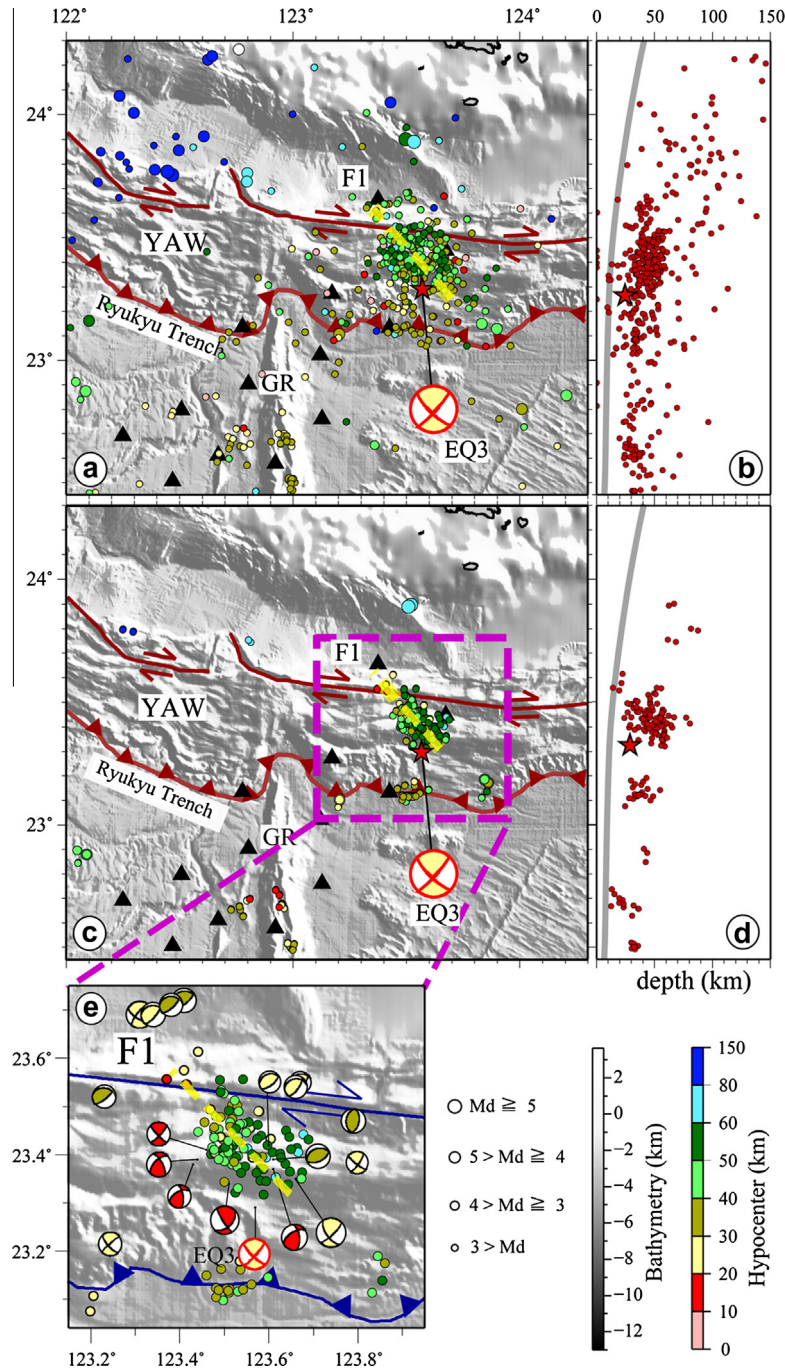
Fig. 3. (a) Hypocenters of 514 earthquakes recorded by the OBS network and (b) their distribution along a N–S cross-section; (c) positions of 336 earthquakes relocated with the HypoDD program (Waldhauser and Ellsworth, 2000) and (d) their distribution along a N–S cross-section. Colors show the earthquakes depth ranges. The gray line in (b and d) shows the plate surface adopted from Font et al. (1999). (e) Focal mechanisms of the aftershocks determined by the Global CMT network in the rectangle area shown in (c) during the recording period of the OBS temporary network. The NW–SE oriented light yellow dashed line F1 represents the ruptured fault zone determined by the aftershocks distribution and focal mechanisms. Black triangles correspond to the locations of OBS stations. Red star shows the main shock of the 17th August 2009 earthquake. The size of dots in (a and c) is function of the magnitude Md. (For interpretation of the references to color in this figure legend, the reader is referred to the web version of this article.)

the difference in travel times for two events observed at one station can be attributed to the spatial offset between the events with high accuracy. This program is especially useful in regions with a dense distribution of seismicity which could be an appropriate method for the observation of aftershock activity. Because the basic assumption of this approach is the small distance between two events, we thus set the maximum hypocentral separation allowed between linked events be 10 km. Then, HypoDD removes data for event pairs with separation distances larger than 10 km for the first

iteration. Thus, we can understand why the subduction events and most events outside the aftershock area are dropped after the application of HypoDD program. In our relocation, the distance between two earthquakes forming a pair was 10 km at the largest, but most of the pairs were approximately 6.14 km, yielding 4875 (P-wave) and 6075 (S-wave) differential travel-time data at 14 stations. The majority of relocated earthquakes range in depth from 10 to 60 km within the subducting PHS plate (Fig. 3c–e). The earthquakes are mostly distributed in a NW–SE direction beneath the
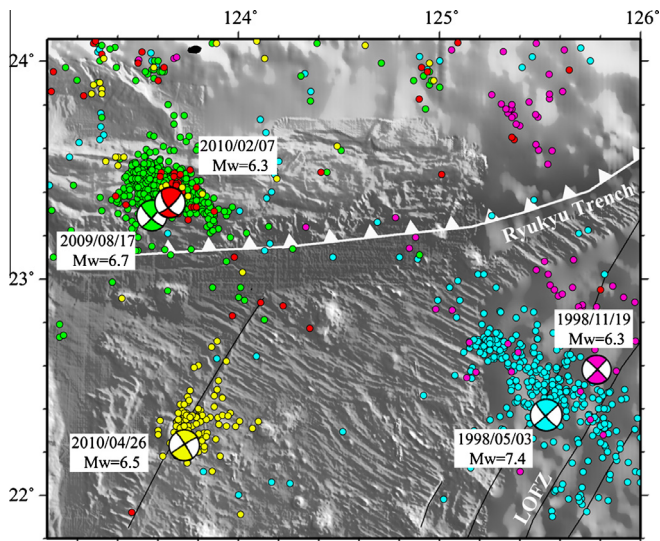
Fig. 4. Focal mechanism of earthquakes with magnitude greater than six determined by Global CMT for the period from 1976 to September 2011 are plotted in different colors. Their aftershocks occurred within one month after its corresponding mainshock are plotted by using the same color. (For interpretation of the references to colour in this figure legend, the reader is referred to the web version of this article.)

Ryukyu accretionary wedge. The orientation of this trend (light dashed yellow line in Fig. 3a, c and e, named F1 hereafter) appears to follow the NW–SE fault plane solution of the Global Centroid Moment Tensor (CMT) focal mechanism (http://www.globalcmt. org/) for the 17 August 2009 Mw 6.7 earthquake (red star in Fig. 3a and c). The focal mechanism also indicates a sinistral rupture along an approximately vertical fault plane for the 17 August 2009 Mw 6.7 earthquake, which is roughly parallel to the PHS/EU convergence direction. The focal mechanism of the strike-slip earthquakes located in the PHS and with magnitude greater than 6.0 and their corresponding aftershocks occurred within 1 month from their mainshock are plotted in Fig. 4 by different color. Firstly, we find similar aftershocks distribution pattern which is consistent with that determined from the OBS network. This observation not only gives evidence for the presence of the NW–SE active feature but also suggests that almost the entire PHS is dominated by similar stress regime.

3. Discussion

As mentioned above, the aftershock distribution suggests a sinistral present-day motion along the fault F1. Several previous studies proposed that the compressional and extensional stresses dominating the Ryukyu subduction system are induced by the oblique subduction of the PHS/EU. In this context, the origin of the F1 strike-slip feature is unclear. In light of the available geophysical data (Fig. 5), we will discuss the nature of this feature.

3.1. Magnetic and gravity anomaly patterns

Due to the fact that most sedimentary rocks and surface-cover formations (including water) are effectively nonmagnetic, the observed magnetic anomalies are generally attributable to the underlying igneous and metamorphic rocks, even where they are concealed from direct observation at the surface. Anomalies arising from the magnetic basement are only diminished in amplitude and extended in wavelength through the extra vertical distance between source and magnetometer imposed by the nonmagnetic

sediment layers. Gravity anomalies are local variations in gravity that result from topographic and subsurface density variations. Thus, both magnetic and gravity anomaly data could be helpful for the determination of geological structures. Sometimes it may be difficult to illustrate the tectonic structures for a already subducted plate due to the complicated subduction system process on its top, including volcanic arc, backarc basin activity etc. However, the observation on the oceanic plate which has not yet been subducted could also provide some information. Fig. 4c shows magnetic anomalies draped on the bathymetric map. Separated from the West Philippine Basin by the Gagua Ridge (GR), the Hua-tung Basin (HB) displays several E–W trending magnetic lineations and two N–S trending fracture zones (Deschamps et al., 2000; Hsu et al., 1996). Northeast of segment F2 (light gray line in Fig. 2a), the E–W trending magnetic reversal pattern is absent (Deschamps et al., 2000; Hsu et al., 1996). In contrast, east of the Gagua Ridge, the F1 and F2 (light gray dashed line in Fig. 5a–c) appear to extend southeastward and outline a domain of high magnetic anomalies (Fig. 5c). In addition, F1 and its western extension roughly bound the low gravity anomaly zone in the east (Fig. 5b). We suggest this main magnetic and gravity gradient is associated with a major tectonic boundary and/or a former transform fault, which could preferentially rupture. Lallemand et al. (2001) have proposed a tear fault in the upper plate (Eurasian Plate), along this sharp gravity gradient. However, in our study, the relocated earthquakes are mainly distributed within the lower plate (Philippine Sea Plate) which indicates that the rupture occurred the subducting plate.

3.2. Rupture distribution

3.2.1. Northern extend of the rupture

The existence of F1 beneath the southwestern Ryukyu accretionary wedge is illustrated by the aftershock distribution. Moreover, several strike-slip earthquakes located to the northwest of the aftershock cluster provide evidence of the northwestward prolongation of F1 to northern Taiwan (Fig. 5a). With a detailed examination of local seismicity and source parameters of 62 recent earthquakes first analyzed by Kao et al. (1998b), the locations of several strike-slip events are exactly along the NW prolongation of F1. Similarly, a recent strike-slip earthquake, with Mw 4.49 and a focal depth of 76 km (30 April 2011 beneath northeastern Taiwan), also coincides with the trace of F1 (EQ4, green line beach ball in Figs. 1, 5a and d). Based on seismic tomographic results, the possible western edge of the slab is identified in terms of a stripe of low Vp and Vs, and Vp/Vs ratio greater than 1.78 beneath northern Taiwan (Lin et al., 2004) (red zones in Fig. 5d). Areas of high Vp/Vs anomalies, interpreted as the dehydration processes from subducting sediments, oceanic crust, and serpentinized mantle, are located above the western edge of the Ryukyu slab and are consistent with the western termination of slab contours. To the north of F1, the anomalous high Vp/Vs zones change orientation from N–S to NW–SE, which implies that the slab is not only deeper to the north of F1 but also has a sinistral motion along F1. It is also noted that the slab contours (black dashed lines in Fig. 5) deflect along the NW prolongation of F1 (Fig. 5).

3.2.2. Southern extent of the rupture

Previous discussions suggest that the NW–SE trending rupture of the PHS plate propagates as far as the western edge of the Ryukyu slab and also to 123.6°E in a southeastward direction (Fig. 2). Indeed, farther southeast, five strike slip earthquakes are located at approximately 125.5°E and 22.5°N, immediately west of the Luzon-Okinawa fracture zone (LOFZ), and another earthquake is located east of the LOFZ (Fig. 1); these earthquakes have approximately the same focal mechanisms as those of the 17 August 2009 earthquake (Fig. 1) and their aftershocks distribution is
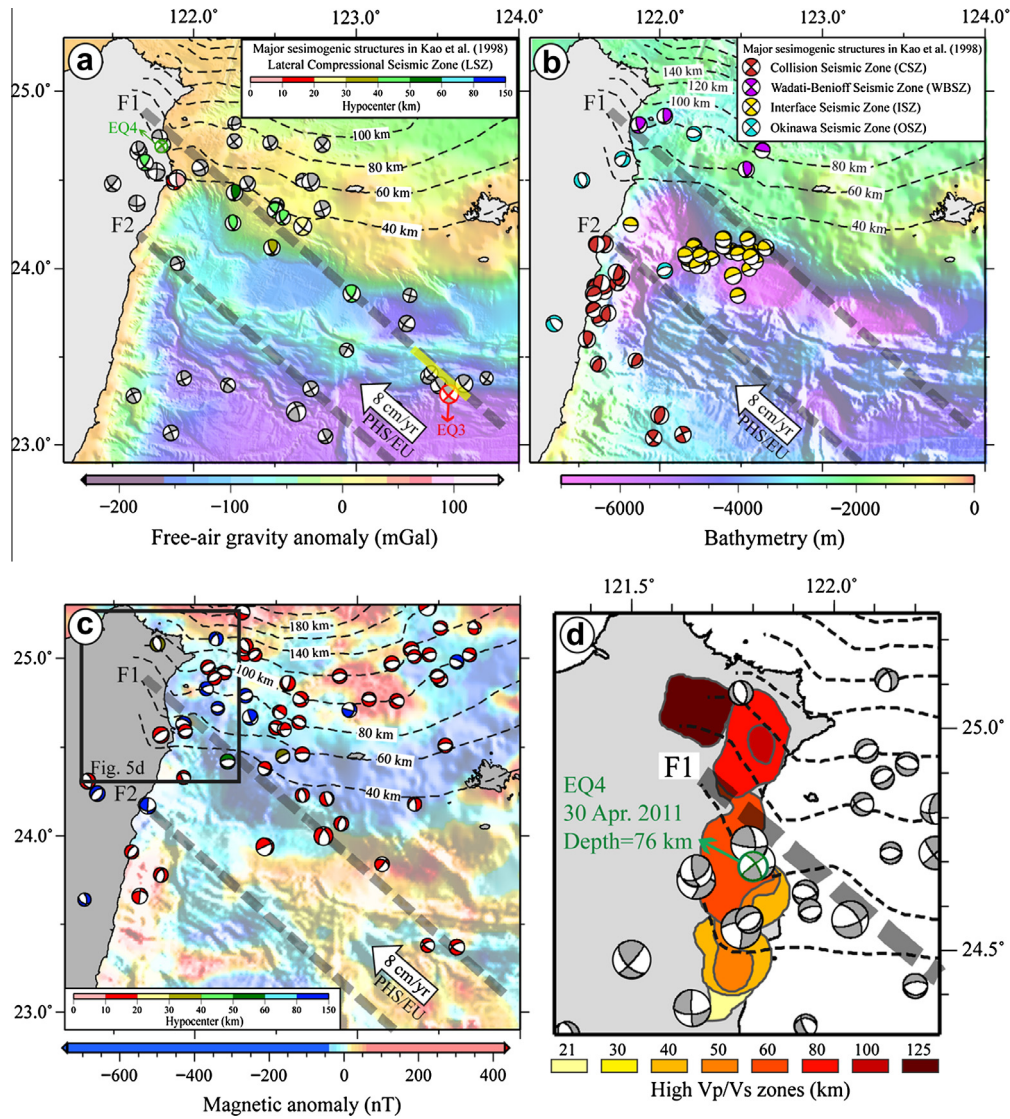
Fig. 5. Bathymetric (Chang, 2007) (a), free-air gravity anomaly (b), magnetic anomaly (c), maps (Hsu et al., 1998) and seismic tomographic results (Lin et al., 2004) (d) in the western Ryukyu subduction zone area. The gravity and magnetic anomalies are draped on the bathymetric map. In (a) gray spheres show the focal mechanisms from the Global CMT catalog between January 1976 and September 2010. Only strike-slip focal mechanisms are plotted. Colored spheres show the focal mechanisms determined by Kao et al. (1998b) for the seismogenic structure "Lateral Compressional Seismic Zone (LSZ)". The green line sphere shows the 30 April 2011 (Mw = 4.49, depth = 76 km) strike-slip earthquake recorded by the BATS (Broadband Array in Taiwan for Seismology) network (http://bats.earth.sinica.edu.tw/). The red line sphere indicates the 17 August 2009 mainshock. The light yellow line F1 corresponds to the rupture zone of the 17 August 2009 earthquake determined from the relocated aftershocks. In (b), focal mechanisms for other four seismogenic structures determined in Kao et al. (1998b) are shown. The distribution for different seimogenic zones appears to be controlled by the F1 and F2 features. (c) Focal mechanisms from the Global CMT catalog between January 1976 and September 2010. Only normal faulting focal mechanisms are plotted. The colors indicate the earthquake depth range. (d) Geographical distribution of areas with Vp/Vs values higher than 1.78 and low Vp and Vs values (Lin et al., 2004). Areas of high Vp/Vs anomalies are located above the western edge of the Ryukyu slab and are consistent with the western termination of slab contours. The light dashed gray line indicates the possible prolongation of the F1 feature, based on the presence of a series of strike-slip earthquakes shown in Fig. 1. F2 represents a second possible tectonic boundary determined from magnetic anomaly data. Black dashed lines show the slab isobaths determined from the relocated earthquakes (Font et al., 1999). (For interpretation of the references to color in this figure legend, the reader is referred to the web version of this article.)

characterized by similar orientation (Fig. 4). A KAIKO dive performed at the location of one of these earthquakes (3 May 1998 at 22.4°N, 125.6°E, Mw 7.5) found an NW–SE swath-bathymetric feature, devoid of sediments and with a manganese crust (Matsumoto et al., 2001), which supports the notion of a NW–SE trending rupture along a left-lateral strike-fault plane. Thus, F1 could extend more or less from the western edge of the Ryukyu slab to the LOFZ, over a distance of ~500 km.

Following the discussion above, a crucial question should be raised: how an Mw = 6.7 earthquake can rip a rupture over a distance of 500 km? Based on the analysis on the seismic activity in the PHS, the migration of strike slip events in function of time and space is observed. Firstly, an event of Mw = 7.5 occurred in

the vicinity of LOFZ in 1998. Then, the position of hypocenter migrated northwesternward to the Ryukyu forearc area in 2009. Finally, the hypocenter was located in the east of the Gagua Ridge in 2010. This migration of earthquakes infers a stress transfer mechanism propagated within the PHS. Thus, we suggest that the NW–SE feature may be segmented and each part of it could be ruptured at different time period by the occurrence of earthquakes.

3.3. Formation mechanisms

What mechanism could cause the NW–SE left-lateral tearing of the northwestern part of the PHS plate along F1? Fig. 6 is a
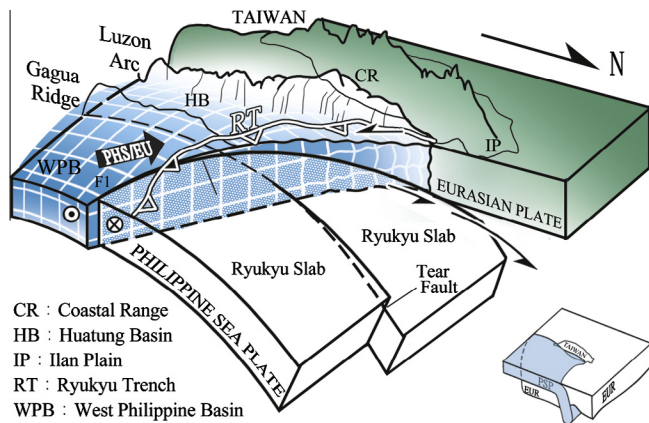
Fig. 6. Geodynamic sketch of the northwestern corner of the Philippine Sea Plate with a portion of the EU plate located above the Ryukyu slab and bounded to the south by the Ryukyu trench (shown in the small diagram) removed for clarity. The left-lateral shear fault F1 offsets the Ryukyu slab and is sub-parallel to the PHS/EU convergence vector. The NS Ryukyu slab tear located along trend from the Gagua Ridge accommodates a downward shift of the western part of the Ryukyu slab.

sketch of our proposed model for the tectonic setting in the NW corner of the PHS plate (with a portion of EU plate above the Ryukyu slab removed for clarity). North of F1, the 123°N tear fault is situated along the trend from the Gagua Ridge (Lin et al., 2007; Sibuet et al., 1998) with a portion of the slab deeper on the western side. Because the direction of F1 is sub-parallel to the N310° direction of PHS/EU convergence, the initiation and growth of this tear fault may be linked to the major tectonic stress of the PHS colliding with the Taiwan orogen in the west, while the PHS slab to the north of F1 is subducting beneath EU. This geodynamic configuration suggests a sharp change in stress regime along F1 as suggested by Wu et al. (2010). Thus, a vertical tear fault may have developed along F1 in addition to the tear fault along 123°E. These two tear faults bound the subducted Ryukyu slab to the west of the Gagua Ridge. This ongoing slab detachment is consistent with the strong decoupling of the plate convergence in this region (Hsu, 2001a). Similarly, the crustal gravitational potential energy loss calculated for the cluster of EQ3 aftershocks implies that extension occurred along the F1 after the mainshock. In fact, Hsu (2010b) proposed the existence of a tear fault along the F2 feature, within the PHS plate, to accommodate the varying PHS plate subduction at an oceanward concave corner. Because a left-lateral motion along F1, sub-parallel to the PHS/EU convergence vector, is associated with a major tectonic stress boundary within the PHS plate, the F2 feature may reveal another complex stress state along the western plate boundary of the PHS. More recently, Wu et al. (2009) proposed a model for the western termination of the Ryukyu subduction zone in which the PHS plate is in compression along the EU plate in the south and central Taiwan, whereas further north, the PHS plate becomes deeper and is no longer in contact with the EU plate. Thus, the state of stress between the PHS and EU plates is different between central Taiwan (where the two plates collide) and northern Taiwan (where the PHS plate subducts below the EU plate). In addition, the minimum principal stress $\sigma 3$ direction computed from the stress inversion of earthquake focal mechanisms (Wu et al., 2010) appears to systematically rotate counter-clockwise from N–S northeast of F2 to NW–SE southwest of F2. Such a pattern might correspond to the interaction between the westward prolongation of the Okinawa trough rifting into northern Taiwan and the tectonic collision in central Taiwan (Kao et al., 1998b; Sibuet et al., 1987).

4. Conclusions

A passive ocean bottom seismometer experiment was conducted, starting three weeks after the 17 August 2009 Mw 6.9 strike-slip earthquake, which was located within the subducting Philippine Sea Plate beneath the southwestern Ryukyu accretionary wedge. The NW–SE elongated distribution of 336 relocated aftershocks suggests a NW–SE left-lateral fault rupture (F1) within the subducting PHS plate. Available geophysical data show that this fault is an important tectonic boundary and probably extends to the western edge of the Ryukyu slab. West of F1, the PHS is directly in compressional contact with the Taiwan orogen, but the border of the PHS plate gradually deepens northward and finally subducts beneath the EU plate. Thus, the state of stress between the PHS and EU plates is different from south to north Taiwan. In south to central Taiwan, the two plates collide where as in northern Taiwan, the PHS plate may freely move below the EU plate. This mechanism could explain the left-lateral motion, sub-parallel to the PHS/EU convergence vector, along F1.

References

Auffret, Y., Pelleau, P., Klingelhoefer, F., Géli, L., Crozon, J., Lin, J.-Y., Sibuet, J.-C., 2004. MicrOBS: A new generation of ocean bottom seismometer. First Break 22, 41–47.

Chang, C.-M., 2007. Seafloor structures in western West Philippine Basin. Master thesis, Institute of Geophysics, National Central University, Taiwan, 42 pp (in Chinese).

Deschamps, A., Monie, P., Lallemand, S., Hsu, S.K., Yeh, K.Y., 2000. Evidence for early cretaceous oceanic crust trapped in the Philippine sea plate. Earth Planet Sci. Lett. 179, 503–516.

Font, Y., Lallemand, S., Angelier, J., 1999. Transition between the active orogen of Taiwan and the Ryukyu subduction: new insight from seismicity. Bull. Soc. Geol. Fr. 170, 271–283.

Hayes, G.P., Briggs, R.W., Sladen, A., Fielding, E.J., Prentice, C., Hudnut, K., Mann, P., Taylor, F.W., Crone, A.J., Gold, R., Ito, T., Simons, M., 2010. Complex rupture during the 12 January 2010 Haiti earthquake. Nat. Geosci. 3, 800–805.

Hsu, S.K., 2001a. Lithospheric structure, buoyancy and coupling across the southernmost Ryukyu subduction zone: an example of decreasing plate coupling. Earth Planet Sci. Lett. 186, 471–478.

Hsu, S.K., 2001b. Subduction/collision complexities in the Taiwan-Ryukyu junction area: tectonics of the northwestern corner of the Philippine Sea Plate. Terr. Atmos. Oceanic Sci. 12, 209–230.

Hsu, S.K., Liu, C.S., Shyu, C.T., Liu, S.Y., Sibuet, J.C., Lallemand, S., Wang, C.S., Reed, D., 1998. New gravity and magnetic anomaly maps in the Taiwan-Luzon region and their preliminary interpretation. Terr. Atmos. Oceanic Sci. 9, 509–532.

Hsu, S.K., Sibuet, J.C., Monti, S., Shyu, C.T., Liu, C.S., 1996. Transition between the Okinawa trough backarc extension and the Taiwan collision: new insights on the southernmost Ryukyu subduction zone. Mar. Geophys. Res. 18, 163–187.

Kao, H., Huang, G.C., Liu, C.S., 2000. Transition from oblique subduction to collision in the northern Luzon arc – Taiwan region: constraints from bathymetry and seismic observations. J. Geophys. Res. 105, 3059–3079.

Kao, H., Jian, P.R., 2001. Seismogenic patterns in the Taiwan region: insights from source parameter inversion of BATS data. Tectonophysics 333, 179–198.

Kao, H., Jian, P.R., Ma, K.F., Huang, B.S., Liu, C.C., 1998a. Moment-tensor inversion for offshore earthquakes east of Taiwan and their implications to regional collision. Geophys. Res. Lett. 25, 3619–3622.

Kao, H., Shen, S.S.J., Ma, K.F., 1998b. Transition from oblique subduction to collision: earthquakes in the southernmost Ryukyu arc-Taiwan region. J. Geophys. Res. 103, 7211–7229.

Kubo, A., Fukuyama, E., 2003. Stress field along the Ryukyu Arc and the Okinawa Trough inferred from moment tensors of shallow earthquakes. Earth Planet Sci. Lett. 210, 305–316.

Lallemand, S., Font, Y., Bijwaard, H., Kao, H., 2001. New insights on 3-D plates interaction near Taiwan from tomography and tectonic implications. Tectonophysics 335, 229–253.

Lin, J.Y., Hsu, S.K., Sibuet, J.C., 2004. Melting features along the western Ryukyu slab edge (northeast Taiwan): tomographic evidence. J. Geophys. Res. 109. http://dx.doi.org/10.1029/2004JB003260.

Lin, J.Y., Sibuet, J.C., Lee, C.S., Hsu, S.K., Klingelhoefer, F., 2007. Origin of the southern Okinawa Trough volcanism from detailed seismic tomography. J. Geophys. Res. 112. http://dx.doi.org/10.1029/2006JB004703.

Matsumoto, T., Kimura, M., Nakamura, M., Ono, T., 2001. Large-scale slope failure and active erosion occurring in the southwest Ryukyu fore-arc area. Nat. Hazards Earth Syst. Sci. 1, 203–211.

Nettles, M., Hjorleifsdottir, V., 2010. Earthquake source parameters for the 2010 January Haiti main shock and aftershock sequence. Geophys. J. Int. 183, 375–380.

Sibuet, J.C., Deffontaines, B., Hsu, S.K., Thareau, N., Le Formal, J.P., Liu, C.S., Party, A., 1998. Okinawa trough backarc basin: early tectonic and magmatic evolution. J. Geophys. Res. 103, 30245–30267.

Sibuet, J.C., Letouzey, J., Barrier, F., Charvet, J., Foucher, J.-P., Hilde, T.W.C., Kimura, M., Chiao, L.-Y., Marsset, B., Muller, C., Stéphan, J.-F., 1987. Back arc extension in the Okinawa trough. J. Geophys. Res. 92 (14041–14014), 14063.

Tsumura, K., 1967. Determination of earthquake magnitude from total duration of oscillation.

Waldhauser, F., Ellsworth, W.L., 2000. A double-difference earthquake location algorithm: method and application to the northern Hayward fault, California. Bull. Seismol. Soc. Am. 90, 1353–1368.

Wang, T.K., McIntosh, K., Nakamura, Y., Liu, C.S., Chen, H.W., 2001. Velocity-interface structure of the southwestern Ryukyu subduction zone from EW9509-1 OBS/MCS data. Mar. Geophys. Res. 22, 265–287.

Wu, F.T., Liang, W.T., Lee, J.C., Benz, H., Villasenor, A., 2009. A model for the termination of the Ryukyu subduction zone against Taiwan: a junction of collision, subduction/separation, and subduction boundaries. J. Geophys. Res. 114, B07404.

Wu, W.-N., Kao, H., Hsu, S.-K., Lo, C.-L., Chen, H.-W., 2010. Spatial variation of the crustal stress field along the Ryukyu-Taiwan-Luzon convergent boundary. J. Geophys. Res. 115, B11401.

Yu, S.B., Chen, H.Y., Kuo, L.C., 1997. Velocity field of GPS stations in the Taiwan area. Tectonophysics 274, 41–59.